AIMS Environmental Science, 5(3): 173–194.
DOI: 10.3934/environsci.2018.3.173
Received: 05 February 2018
Accepted: 08 June 2018
Published: 15 June 2018

http://www.aimspress.com/journal/environmental

Research article

Satellite and ground atmospheric particulate matter detection over Tucumán city, Argentina, space-time distribution, climatic and seasonal variability

María E. García[1], Lara S. Della Ceca[2], María I. Micheletti[2,3], Rubén D. Piacentini[2,4], Mariano Ordano[5], Nora J. F. Reyes[1,6], Sebastián Buedo[6] and Juan A. González[6,*]

[1] Laboratory of Palynology, Miguel Lillo Foundation, Miguel Lillo 251, T4000JFE, San Miguel de Tucumán, Tucumán, Argentina
[2] Group of Atmospheric Physics, Solar Radiation and Astroparticles, Institute of Physics Rosario, CONICET—National University of Rosario, 27 de Febrero 210bis, S2000EZP, Rosario, Santa Fe, Argentina
[3] Faculty of Pharmaceutical and Biochemical Sciences, National University of Rosario, Suipacha 531, Rosario, Santa Fe, Argentina
[4] Laboratory of Energy Efficiency, Sustainability and Climate Change, IMAE, Faculty of Exact Sciences, Engineering and Surveying, National University of Rosario, Pellegrini 250, S2000BTP, Rosario, Santa Fe, Argentina
[5] Miguel Lillo Foundation and Lillo Executive Unit (UEL-FML-CONICET), Miguel Lillo 251, T4000JFE, San Miguel de Tucumán, Tucumán, Argentina
[6] Institute of Ecology, Miguel Lillo Foundation, Miguel Lillo 251, T4000JFE, San Miguel de Tucumán, Tucumán, Argentina

* **Correspondence:** Email: jalules54@gmail.com; Tel: +543814231860.

Abstract: The analysis of atmospheric particles (aerosols) is of special interest due to their potential effects on human health and other applications. In this paper the climatic and seasonal effects on aerosols have been characterized in Tucumán city (26°50' S, 65° 13' W, 450 m asl), Argentina, for the 2006–2013 period. The atmospheric aerosols in Tucumán city result from both stationary and mobile sources such as: industrial activity of sugar cane and alcohol distilleries, paper industry, biomass burning (mainly sugarcane waste crop and grasslands), household waste burning and transport emissions. The peak of industrial activity is seasonal, coincident with the austral winter (July-August-September), when accumulation of particles in the lower atmosphere occurs. In this

region, there are no studies like the present one that evaluate, using "*in situ*" equipment, the temporal variation of aerosols and its causes, by applying modern analytical techniques. A continuous volumetric and isokinetic sampler of Hirst type (Burkard), was used for atmospheric particle sampling, in weekly records between 2006 and 2013. The particle concentration (number of particles per cubic meter) showed an increasing trend in the studied period. The monthly variation of: the particle concentration; the aerosol optical thickness at a wavelength of 550 nm (AOD_{550}) obtained from the Moderate Resolution Imaging Spectroradiometer (MODIS) sensors onboard Aqua (NASA) satellite, and the AOD from different aerosol tracers (black and organic carbon, sea salt, sulfates, dust) obtained from the Modern-Era Retrospective Analysis for Research and Applications (MERRA-2), were also analyzed. The temporal variation in particle concentration was explained mostly by wind direction, while the corresponding variation for AOD_{550}(MODIS) was explained by temperature and seasonality (as by-product of climatic variation and anthropogenic particle emission sources). The variation in the AOD_{550}(MERRA-2) data series were explained by temperature, humidity, precipitation, and seasonality, with less effect of wind speed and direction. Particle concentration, AOD_{550}(MODIS), and AOD_{550}(MERRA-2) were highly variable. The cross-correlation between AOD_{550}(MODIS) and AOD_{550}(MERRA-2) time series was significantly positive at lag zero. Other contribution was the determination of the space-time distribution of aerosols on a monthly basis considering AOD_{550} MODIS (3 km × 3 km) data. The present study suggests that these variables are affected by temperature and wind dynamics driven by seasonal and high-order autoregressive non-linear processes.

Keywords: Remote sensing; air pollution; seasonality; particulate matter quantification; environmental monitoring

1. Introduction

Atmospheric particles (aerosols) are of special interest to environmental sciences due to their potential effects on human health and the ecosystem [1–6]. According to their equivalent aerodynamic diameter, the particles are classified as: coarse (PM_{10}: equal or smaller than 10 μm), fine ($PM_{2.5}$: equal or smaller than 2.5 μm) and ultrafine ($PM_{0.1}$: equal or smaller than 0.1 μm). The atmospheric distribution of particles is determined by the location of the sources and the climatic conditions. Most studies that correlate aerosols with meteorological conditions have been carried out in the Northern Hemisphere [7–10]. In South America this topic is still highly unexplored and scarce data are available [7,8,11–17]. Consequently, every step for understanding aerosol dynamics is important for guiding management environmental policies and their relationship with climate change.

Due to the fact that anthropogenic aerosols are generally emitted at essentially surface level and remain strongly constrained in the planetary boundary layer (PBL), the air pollutants are significantly higher in the PBL than in the rest of the atmosphere [18,19]. Approximately 95% of the total atmospheric particles are concentrated in the PBL [20]. Due to the air mass convective movements within an average boundary layer, the air can be considered to be well mixed. However, local meteorological conditions within the boundary layer can affect the altitudinal distribution of aerosols due to mixing variations. Particulate concentration at ground level depends on boundary layer thickness, which is also affected by variables such as temperature [21].

San Miguel de Tucumán city, located in the Northwest of Argentina, is the most densely populated place in Tucumán province (~64 inhabitants/km^2; 794,327 inhabitants in 2010, Source: INDEC/Instituto Argentino de Estadísticas y Censos). Due to that, high levels of particulate matter concentration may have a considerable impact on human health and environmental quality. Atmospheric aerosols in San Miguel de Tucumán are originated from several sources, such as industrial activity (sugarcane and alcohol distilleries, paper industry), biomass burning (sugarcane waste, grasslands and solid urban waste) and transport emissions [22]. These activities cause the accumulation of aerosols in the lower atmosphere, producing *Atmospheric Brown Clouds* (ABC), a dense blanket of polluted air consisting of an unhealthy mix of ozone, smoke and other particles produced by human activities (see for example the NASA URL: www.nasa.gov/vision/earth/environment/brown_cloud.html). These clouds produce significant variation in the Aerosol Optical Depth (AOD), aerosol index (AI) and total solar irradiance (TSI) [22]. The peak of sugarcane harvest, burning, and industrial activity, occurring mainly during the austral winter (July to September) leads to the generation of ABC [22]. This phenomenon also occurs in other regions of Argentina, as well as in the neighboring areas of Paraguay, Bolivia and Brazil. However, it must be pointed out that in the area investigated in this work, there are no other studies like the present one that evaluate, using "*in situ*" equipment, the temporal variation of aerosols and its causes, by applying modern analytical techniques.

The dynamics of particulate matter in San Miguel de Tucumán is highly seasonal, with two periods of high concentration in correspondence with the climatic seasonality and anthropogenic particle emission sources [22]. During the austral winter, the harvest of sugarcane and citrus is performed with high consumption of liquid fuels (gas oil, fuel oil) and bagasse sugarcane is used to generate caloric energy for boilers. The boilers burn approximately 4,000,000 tons of bagasse per year. Since combustion is incomplete, this practice generates approximately 90,000 tons of solids (soot) per year (Environment Secretary of Tucumán, *unpublished data*). Since 2010, Scrubber type filters on the boilers have been employed in order to reduce air contamination. Even if particles larger than 2.5 microns are filtered, the smaller particles continue being released into the low atmosphere. This fine fraction is the most harmful to human health, being present in the interchange of gases between different regions of the lungs [3]. Other sources of atmospheric aerosols emitted by the sugarcane agro-industry are: the burning of sugarcane fields prior to harvest, the machine displacement and the transport of sugarcane. These activities take place during the dry season (May to October), when the almost absence of rainfall reinforces the accumulation of particulate matter suspended in the air. Moreover, other sources of air pollution are forest biomass burning [23], burning of solid urban waste, industries (electric energy generation from natural gas, paper mill, metalworking and food processing) and vehicular emissions (apart from sugarcane activity). These activities also contribute to the production of the ABC above described. During the austral summer (December to March), the activity of the sugarcane industry is low and the precipitation levels increase, leading to the washing of atmospheric aerosols and to a decrease or vanishing of the ABC. The anthropogenic aerosol sources vary along the seasons, so a seasonal dependence of particle concentration is expected.

The complexity of San Miguel de Tucumán atmospheric dynamics is also enhanced by topographic effects [22]. The territory is divided into plains in the East (200 to 400 m asl), foothills and mountains of low height in the center-West and a chain of high mountains to the West (5500 m asl) [24]. The prevailing winds come mostly from Southwest and Northeast sectors, and are affected by local

topography [25,26]. The combination of topography and the wind pattern, produce an air particulate accumulation in the central area of the province, where San Miguel de Tucumán city is located. Due to the relatively high population density, high levels of particulate matter concentration may have a considerable impact on human health and environmental quality. The objectives of this work are: (1) To describe the space-time distribution of suspended particles in San Miguel de Tucumán city and its surroundings; (2) To explore the possible correlation between particle concentration measured *in situ* and the AOD estimated by satellite sensors; (3) To determine the influence of local climate variables and seasonality on the temporal variation in particle concentration and AOD.

2. Materials and methods

2.1. Area of study and particulate sampling

Between September 2006 and August 2013, atmospheric aerosols were collected in San Miguel de Tucumán city, Argentina. The particles were captured on a weekly basis by a continuous volumetric and isokinetic sampler of Hirst (1952) type [27], Burkard model, installed on the roof of the Botany building of the Fundación Miguel Lillo (26º49'53.19" S, 65°13'18.74" W, 452 m asl). The air stream (air flow of 10 L/min) entering the device with the load of atmospheric particles, impinges on a transparent tape (Melinex) impregnated with a silicone solution. The aperture of the device is 14 mm width and 2 mm height. As the sampler does not include a particle filter, particles of all sizes remain captured in the tape. The sampler operates driven by a watch system that synchronizes the time exposure of the different portions of the tape, while it rotates during a weekly period**.** The tape was removed every seven days and cut into fragments, each one corresponding to a daily period, following the recommendations done by the Aerobiology Spanish Network (Red Española de Aerobiología) [28]. Each daily fragment was mounted on a slide and photographed under a Carl Zeiss Axiostar Plus (100X objective) microscope equipped with Canon PowerShot A620 digital camera 7.1 MP and a scale in microns. Since the sensor is a Burkard continuous collector, a huge amount of data would be available, but makes our sampling approach impractical. So, we selected a fraction of the one-day collection tape corresponding to the Sunday day at 22:00 hours (local time = Universal Time − 3 hours) up to 23:00 hours, hereafter referred as *sample*. This time period represents the baseline situation for the aerosol content in the atmosphere, as due to the reduced traffic of vehicles and other activities (from construction, roadwork, and other activities mentioned in the Introduction section), it can be assumed that the anthropogenic aerosols reach their lower limit on Sunday night. So, the present results show the baseline situation for aerosols along the seasons at Tucumán. However, the aerosol values at rush hours during working days are expected to surpass the values here reported.

Photographs of the samples were processed using the ImageJ software 1.4 g version [29], in order to determine the number and the area of the particles for each sample. The area of the particles is given in units of surface (μm^2). The particle concentration (in particles/m^3) was estimated by analyzing the photographs, taking into account the number of particles counted in the observed area of the sample, the air flow of the instrument, the dimensions of the tape (being its width 14 mm, completely exposed to the incoming air containing the aerosols, at every measurement time) and the rotation velocity of the tape fixed by the internal clock of the instrument (corresponding to a displacement of 2 mm per hour, along the tape length). The resulting formula is:

$$C = \frac{14 * \mathrm{NCP}}{PA * 0.3} [\frac{mm^2}{m^3}] \quad (1)$$

where 14 corresponds to the band width, NCP is the number of counted particles in each photograph, PA is the observed area of the sample in the corresponding photograph and 0.3 is a factor that arises when taking into account the air flow of the instrument and the rotation velocity of the tape.

In the present work, particle concentration values are reported as monthly averages from the weekly samples. Due to a failure in the sampling instrument, the samples obtained from February to April 2010 period were not considered. So, to fill these missing data in the time series analysis, the historical average of the corresponding month was employed [30,31]. In order to test the influence of this replacement in the final results, a moving average was used and the analysis resulted in similar outputs.

2.2. Meteorological dataset

Daily climate data (air temperature, relative humidity, wind direction, wind speed, precipitation) were obtained from Argentina National Meteorological Service (SMN, www.smn.gov.ar). In particular, the accumulated precipitation per month was obtained.

2.3. Aerosol Optical Depth

Aerosol Optical Depth (at a medium visible range wavelength of 550 nm; AOD_{550}) was obtained from the Moderate Resolution Imaging Spectroradiometer (MODIS; https://modis.gsfc.nasa.gov/) aboard Aqua/NASA satellite (passing time of Aqua satellite in the interval 1–5 p.m. local time). The MODIS instrument provides high radiometric sensitivity (12 bit) in 36 spectral bands ranging in wavelength from 0.4 μm to 14.4 μm. The Dark Target algorithm uses MODIS bands 1 through 7 and 20 (prior cloud screening using MODIS data) to retrieve AOD over oceans and land. In this study we used the MODIS dataset from collection 6, which, in addition to the AOD product of 10 × 10 km of spatial resolution, provides an AOD product with a spatial resolution of 3 km × 3 km, unlike the deep blue algorithm that only offers a product of 10 km × 10 km of spatial resolution. Over land, the dynamic aerosol models are derived from ground-based sky measurements and used in the net retrieval process [32]. The 3 km × 3 km spatial resolution provided by the MYD04_3K AOD product enables us to make a first approach to aerosol space-time distribution in Tucumán city and its surroundings. This higher spatial resolution, with respect to other available AOD satellite products, is more suitable for air quality studies at a major scale and a potential tool to detect aerosol sources. A total of 2554 daily AOD-Aqua products were processed corresponding to the 1st September 2006–31th August 2013 period.

MODIS data, unlike ground-based stations, provide information on large regions and enables us to study aerosols not only at San Miguel de Tucumán city but also at nearby urbanizations such as Tafí Viejo (point 2 in Figure 1), Alderetes (point 3), Banda del Río Salí (point 4), San Pablo (point 5) and Lules (point 6) with an acceptable spatial resolution. In correspondence with the in-situ measurements, AOD satellite data are considered only for Sunday days.

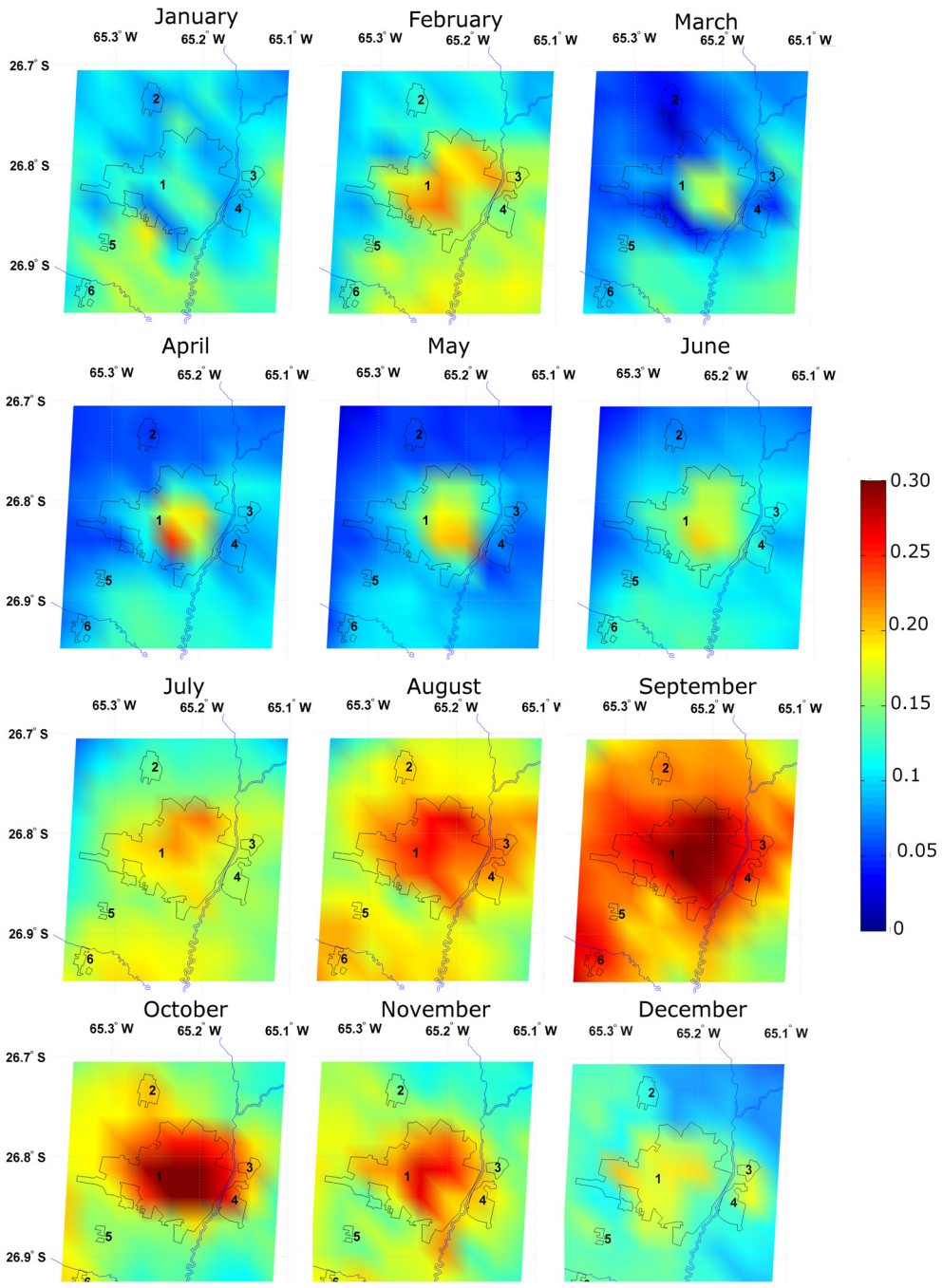

Figure 1. False color maps of monthly AOD_{550} determined with the Dark Target algorithm based on MODIS Aqua/NASA (2006–2013) data, of Tucumán city and adjacent cities, indicated as follows: Tucumán city (point 1), Tafí Viejo (2), Alderetes (3), Banda del Río Salí (4), San Pablo (5) and Lules (6). Black lines indicate the cities boundaries. Blue lines indicate the main rivers and streams in the area.

2.4. Aerosol Optical Depth by aerosol type

To determine the composition of atmospheric aerosols and evaluate its correlation with particulate matter collected at Tucuman city, we used the Modern-Era Retrospective analysis for

Research and Applications version 2 (MERRA-2) [33] on a monthly basis. MERRA-2 is a NASA atmospheric reanalysis for the satellite era using the Goddard Earth Observing System Model, Version 5 (GEOS-5) with its Atmospheric Data Assimilation System (ADAS), version 5.12.4. This model focuses on historical climate analyses for a broad range of weather and climate time scales and places the NASA EOS suite of observations in a climate context. From this dataset we obtained the monthly AOD at 550 nm average corresponding to total AOD, black carbon (BC), organic carbon (OC), sulfates (SU) and dust (DUST), for the pixel corresponding to the sampling site with a spatial resolution of 0.5° × 0.625° (approximately 56 km × 70 km), from the web: https://giovanni.gsfc.nasa.gov.

3. Data analysis

3.1. Series description at regional and local scale

Space-time variation of AOD was described on a monthly basis for the 2006–2013 period, for latitudes in the 26.68° S–26.95° S range and longitudes in the 65.11° W–65.37° W range. Also, the fluctuations, peaks and temporal profile of particle concentration and AOD_{550}(MODIS) and AOD_{550}(MERRA-2), were characterized. The time profile was explored graphically, applying a *loess* function with a length equal to the span of the series divided by seven (i.e., representing an annual moving average, since 7 years of data are considered). The temporal trend was analyzed by simple linear regression between each response variable, particle concentration or AOD and time (adjusted R^2 are reported). These variables were transformed as *log* (variable) to stabilize the variance and to improve the distribution of model errors.

In addition, the particle concentration trend over the studied period was also evaluated by the Theil-Sen method [34,35]. Briefly, given a set of n (x, y) pairs, the slopes between all pairs of points are calculated. The Theil-Sen estimate of the slope is the median of all these slopes. The advantage of employing the Theil-Sen estimator is that it tends to yield accurate confidence intervals even with non-normal data and heteroscedasticity (non-constant error variance). Because seasonal effects can be important for monthly data, data is first deseasonalised by developing seasonal trend decomposition using loess. In this way, a clearer indication of the overall trend on a monthly basis is provided. The uncertainty in the slope is estimated by running simulations.

3.2. Cross correlation between AOD and particle concentration

Cross-correlation analysis was made between the AOD filtered series and particle concentration. The use of filtered series avoids spurious influences arisen from autocorrelated structure of time series, since the value of a variable X at time t_0 depends on the value of X at time t_{-1}. Filtered series represent the essential variability (standard with white noise). As a consequence of this approach, results of cross-correlation on filtered series are interpreted as the covariation between their temporal dynamics, after controlling for auto-regressive processes. In order to obtain the corresponding stationary filtered series, we used generalized least squares with correlation Auto-Regressive Moving Average (ARMA) structure (1,0) for the particle concentration, and AOD series [36].

The lack of significance in the autocorrelation function (ACF), at maximum lag, was considered as a criterion for model selection, those with non-significant errors in the ACF were selected.

Significant cross-correlation between two series at a given lag means that the variation in the series response (i.e., particle concentration) covaries with lagged series (thus, AOD for the given lagged period [36]). Cross-correlations to lag 12 were selected, because the most important correlations should occur between years. In this way our analytical approach can detect second order influences or even those of higher order up to an annual cycle. In our case, these temporal influences depend on atmospheric processes acting on climate at time scales larger than one month, such as seasonal or annual effects.

3.3. Influence of climate factors on AOD and particle concentration

To assess the influence of local climate factors on particle concentration and AOD, generalized least squares (GLS) models were applied [37–40]. These tools permit the characterization of the structures of variance and error, which is crucial for dealing with typical autoregressive process time series [37]. The first step in building the model was to evaluate the generalized variance inflation factor (GVIF) adjusted by the dimension of the confidence ellipsoid (as GVIF^[1/(2*degrees of freedom)]; [41]) from a linear model with the following factors: season, air temperature, relative humidity, atmospheric pressure, wind speed, wind direction (circular data) and precipitation. Values of adjusted GVIF showed that collinearity among variables is acceptable (GVIF= 1.1 to 2.9 for all variables). Consequently, the initial model was built as:

$$\textit{Variable Response (particle concentration or AOD)} = f(\textit{Season, Temperature, Humidity, Wind speed, Wind direction, Precipitation}) \quad (2)$$

The temporal correlation structure was (1,0) for particle concentration and AOD series. The alternative model includes a variance structure corresponding to different error variances between seasons. This modification considers the heterogeneity of variance resulting from the different seasons. Thus, the model accounts for deviations from homogeneity of variance [40]. To select the model in general, the procedure of Zuur et al. (2009) was used [39]. After each run with maximum likelihood estimates, the optimal model was selected by: (1) comparison of values of Akaike Information Criteria (AIC; the model with the lowest AIC was selected) and (2) inspection of residuals that were validated doing a Shapiro-Wilks test and ACF. White noise in residuals was considered an optimal model. Once the optimal model was selected, the final adjustment was based on restricted maximum likelihood (REML, as indicated in Zuur et al. 2009 [39]). It was applied a generalized additive mixed model (GAMM) [42] with an autoregressive structure of order 1 and a seasonal variance structure as in the AIC model and considering AOD as a covariable. This approach permits an estimation of non-linear relationships (by cubic splines) between the particle concentration and climatic variation and AOD. In this way, we detect the influence of non-linear temporal dynamics. The model was built as:

$$\textit{Particle Concentration} = g(\textit{Season, Temperature, Humidity, Wind speed, Wind direction, Precipitation, AOD}) \quad (3)$$

All the analyses and graphics were performed in R 3.4.1 [43] using the following packages: circular [44], Doby [45], forecast [46], ggplot2 [47], lattice Extra [48], mgcv [49], nlme [50], openair [51] and visreg [52]. The database and R script are available upon request.

4. Results

4.1. Series description at the regional and local scale

4.1.1. Satellite data

Figure 1 shows AOD_{550}(MODIS) monthly mean maps for the studied period (September 2006 to August 2013) over Tucumán city and its surroundings, obtained with MODIS sensor at a 3 km × 3 km spatial resolution, with false colors indicating the intensity of aerosol events. The largest AOD_{550}(MODIS) values are observed from August to November, with a maximum in September-October. Relatively low AOD_{550}(MODIS) values are observed from March to June. The aerosols are mainly concentrated in Tucumán city, indicating and important influence of local sources in the load of particles to the atmosphere. In contrast, the nearby cities show rather low values of AOD_{550}(MODIS) with an increment during spring (September to December). The high AOD values measured in September-October can be explained by the external contribution to the Tucuman city and adjacent regions, due to biomass burning in north of Argentina, Paraguay, Bolivia and Brazil nearest regions [52,53].

Figure 2 presents the monthly mean and standard deviation of the AOD satellite data for the September 2006–August 2013 period and for the corresponding pixel of the in-situ Tucumán city monitoring site (26º49'53.19" S, 65°13'18.74" W). The AOD_{550}(MODIS) mean was 0.224 and presented a 47.07% coefficient of variation (CV).

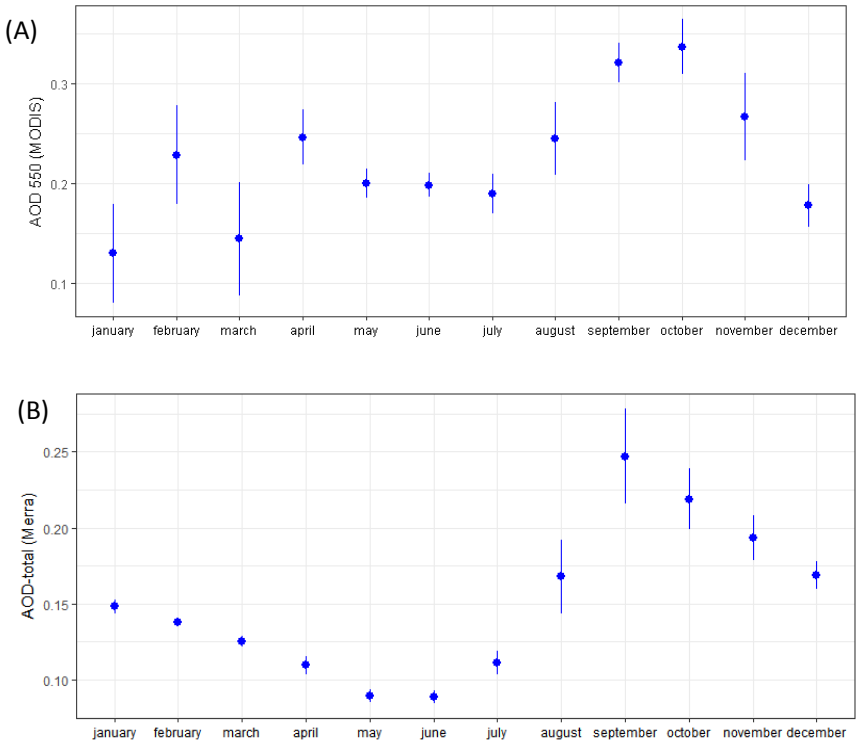

Figure 2. AOD_{550}(MODIS) (A) and AOD_{550}(MERRA-2) (B) monthly mean (point) ± standard error (whiskers) for the September 2006–August 2013 period for the pixel corresponding to the Tucumán city monitoring site (26º 49'53.19" S, 65°13'18.74" W).

The analysis of temporal trend indicates that AOD series are mostly stable in the time window considered (September 2006–August 2013; Figure 3). Coefficients of the linear trend (practically horizontal) of the variables included in the analysis were: MODIS: $R^2 = -0.012$; $F_{1,82} = 0.001$, $p = 0.97$; MERRA-total AOD: $R^2 = 0.013$; $F_{1,82} = 2.068$, $p = 0.1542$; Black Carbon: $R^2 = -0.010$; $F_{1,82} = 0.209$, $p = 0.6486$; Organic Carbon: $R^2 = -0.006$; $F_{1,82} = 0.540$, $p = 0.4646$; Sea Salt: $R^2 = -0.011$; $F_{1,82} = 0.08549$, $p = 0.7707$). However, Sulfates and Dust showed a significantly positive and slow trend through time (Sulfates: $R^2 = 0.038$; $F_{1,82} = 4.303$, $p = 0.04118$; Dust: $R^2 = 0.065$; $F_{1,82} = 6.769$, $p = 0.011$).

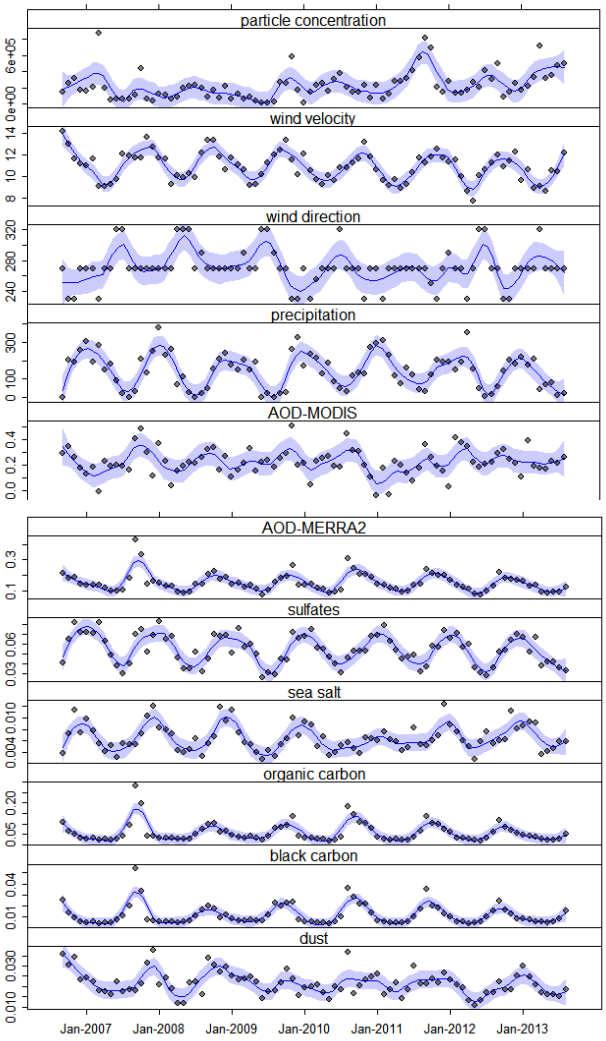

Figure 3. Monthly average values for the September 2006–August 2013 period at the Tucumán city monitoring site (26º49'53.19" S, 65°13'18.74" W) of particle concentration (10^5 particles m^{-3}), wind speed (km per hour), wind direction (degrees), precipitation (mm), AOD_{550}(MODIS), total AOD_{550}(MERRA-2), and aerosol tracers obtained with the MERRA-2 model: sulfates, sea salt, organic carbon, black carbon and dust. The average blue line was adjusted with a (weighted least squares) loess function, with a span of 1/7 and confidence bands with standard error at 0.95 level. Marks on the horizontal axis indicate January of each year.

With respect to aerosol type data, Figure 4 presents the AOD monthly mean and standard deviation for each type of aerosols for the studied period and for the corresponding pixel of the in-situ Tucumán city monitoring site. As expected, during late winter and spring, when biomass burning is more intense in the region (due to sugar cane harvest), a great increase of Organic and Black carbon is observed. Sulfates show also a seasonal behaviour, with higher values during summer and spring, when the temperature and radiation are higher and the formation of secondary aerosols is greater due to atmospheric photochemical processes. Dust have a lower contribution to the AOD in the study area and, as the sulfates, show a seasonal behavior with higher values in summer and spring and lower in autumn and winter. The contribution of sea salt to aod is very small, possibly from long-range atmospheric transport (Figure 4).

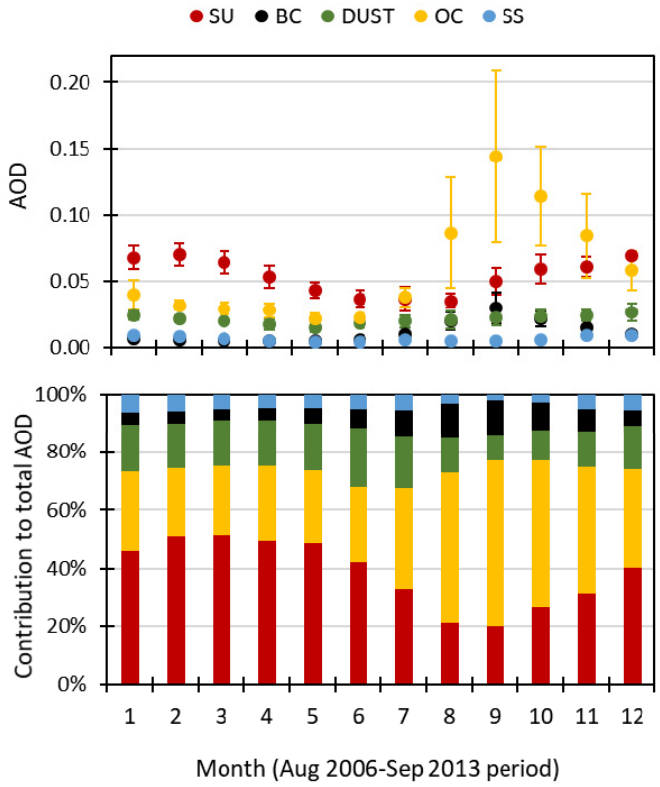

Figure 4. Monthly average and standard deviation of AOD corresponding to different type of aerosols: Sulfates (SU), Black carbon (BC), Dust, Organic Carbon (OC) and Sea Salt (SS), obtained with the MERRA-2 model for the corresponding pixel of the in-situ Tucumán city monitoring site (26º49'53.19" S, 65°13'18.74" W).

4.2. Comparison among measurements of particle concentration, satellite and climate data

Particle analysis collected and measured in Tucumán city showed that 95.9% of them have a diameter smaller than 2.5 μm. The mean value of particle concentration was 2.28×10^5 particles m^{-3} for the whole period and presented a CV of 77.72%. Several high particle concentration values can be observed in Figure 3 top, with the maximum value registered in March 2007 (8.71×10^5 particles m^{-3}). Rather large seasonal variations are also observed in wind and precipitation (Figure 3).

The monthly mean particle concentration for the studied period is presented in Figure 5, where a significant variation in a factor of two from the minimum mean value in February (1.46×10^5 particles m^{-3}) to the maximum mean value in September (2.97×10^5 particles m^{-3}) was observed.

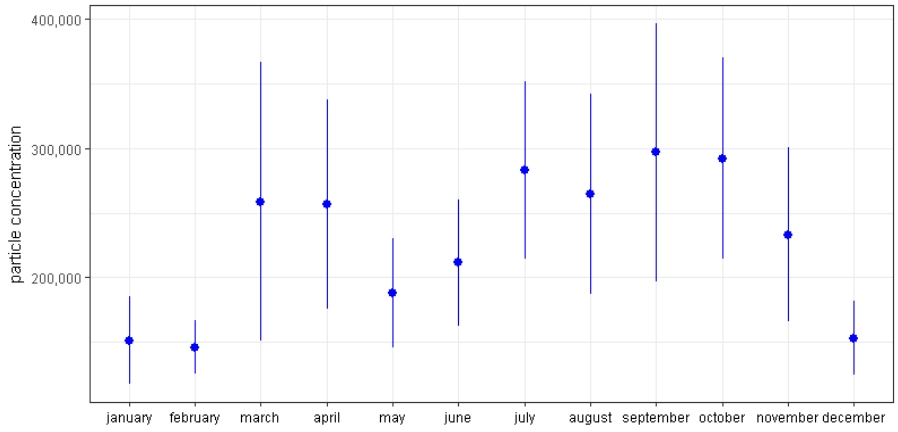

Figure 5. Particle concentration (particle m^{-3}) monthly mean (point) ± standard error (whiskers) for the September 2006–August 2013 period for the pixel corresponding to the Tucumán city monitoring site (26º49'53.19" S, 65°13'18.74" W).

The comparison between the monthly mean particle concentration ground data (Figure 5) and the monthly mean AOD satellite data (Figures 2 and 4) shows that there is a rather good general agreement in the monthly pattern of the aerosol events in the Tucumán city and nearby regions in Spring. During Summer and the first months of Autumn some relative differences can be distinguished between the behaviors of the AOD_{550}(MODIS) data of Figure 2 and of the particle concentrations obtained from the in-situ collection of aerosol samples and their analysis, as shown in Figure 4. These differences could be due to: (a) a possible bias linked to the operational estimation of surface reflectance by the satellite as was reported for Santiago de Chile by Escribano et al. (2014) [13], (b) non-linear relationships between particle concentration at the local level and AOD series. In this way, different relationships might arise depending on seasonal effects.

4.3. Temporal trend in particle concentration

A significant positive trend was observed in particle concentration throughout the studied period, with and increase rate of 2.72×10^4 particles m^{-3} $year^{-1}$. The 95% confidence intervals in the trend ranged between 1.72×10^4 to 4.10×10^4 particles m^{-3} $year^{-1}$. This positive trend is an indication of the increasing contamination by aerosols in Tucumán during the studied period and is a call for the authorities to implement the required policies for protecting the population and for reducing the aerosol emissions.

4.4. Cross correlation between AOD and particle concentration

The cross-correlation analysis between the filtered series AOD_{550} (MODIS) and AOD_{550}(MERRA-2) showed a significant correlation at lag zero ($r = 0.381$, $p < 0.05$; Supplementary,

Figure S1). However, the cross-correlation analysis between the filtered series AOD and particle concentration showed no significant correlation at lag zero between the particle concentration and the lagged AOD_{550} (MODIS) (Supplementary, Figure S2). Considering this result, some sources of uncertainties should be taken into account. First of all, ground-based particle concentration measurements cover a limited spatial range in height, while AOD measures the total particle content of the whole atmospheric column. Considering boundary layer height or particle altitudinal distribution, these variables would help to reduce this uncertainty, but unfortunately no data of this type is available for our area of study and so we cannot explore this matter further. Moreover, ground-based particle concentration measurements have also a limited (local) spatial cover range in the horizontal dimension [55,56]. A greater spatial resolution (of a few kilometers) of the AOD satellite product would better represent the spatial variability of the atmospheric particles [57]. The discrepancies in seasonal patterns between particle concentration and satellite AOD might be attributed to the uncertainties associated with both, the used correlation model and satellite AOD retrievals. Some studies that compare satellite AOD with AERONET AOD observations indicate that the uncertainties in MODIS AOD are proportional to the magnitude of AOD values [33,58]. Therefore, for September and October, the months with higher AOD for the satellite sensor considered in this study, MODIS, would present larger uncertainties.

The cross-correlation analysis between the lagged total AOD_{550}(MERRA-2) filtered series and particle concentration also showed no significant correlation at lag zero (Supplementary, Figure S3). However, when the aerosol type was considered, significant cross-correlations were detected between organic carbon series and particle concentration series at the lags 6 and 11 (Supplementary, Figure S4); and between dust series and particle concentration series at the lags 7 and 10 (Supplementary, Figure S5).

Besides the scale problem associated to particle and AOD measurements, non-linear dynamics might affect the relationship between AOD and particle concentration. This is not directly envisioned by cross-correlations. However, the strong seasonal effects found on AOD series suggest that, when seasonal conditions affect AOD values and distribution, their influence on particle concentration measured at ground would be different depending on the season. This was then confirmed in our non-linear analysis by GAMM (see below).

We like to point out that other works presented also non-correlation results. For example, in the US West, Hu (2009) and Li et al. (2015) [59,60] reported that AOD poorly correlates with $PM_{2.5}$. The first author considers that this difference is mainly due to the difference in terrain, AOD retrieval algorithm and meteorological conditions. The second–authors consider that the seasonally varying mixing height is the primary cause for the AOD and $PM_{2.5}$ discrepancy, in particular, the low AOD but high $PM_{2.5}$ observed during the winter season for Western US. Moreover, van Donkelaar et al. (2006) [61] showed that the relative vertical profile of the aerosol extinction is the most important factor affecting the spatial relationship between the satellite and surface measurements.

4.5. Climate influence

Among the factors we compared, wind direction is the climatic variable most closely related to particle concentration variation. In particular; the fitting of GLS models revealed that wind direction is the most important factor, determining in general negative effects on the monthly variation in particle concentration (Table 1A). As wind direction is measured in circular degrees (in the 0º–360º

range); this result means that a sustained decrease in aerosol concentration is found when the local winds rotate from the SW to the NW direction, as shown in Figure 6. Instead, the variation in AOD_{550}(MODIS), at the ground-based monitor location, is significantly affected by seasonality and temperature (Table 1B). The corresponding partial regressions show large variations in each of the variables, and probably underlying nonlinear dynamics. The most obvious effect is seasonality on the AOD_{550}(MODIS), notably driven by seasonality (autumn and winter changes) and temperature (Figure 6). The AOD_{550}(MERRA-2) variation is significantly affected by seasonality, temperature, humidity, and precipitation (Table 1C; Figure 6).

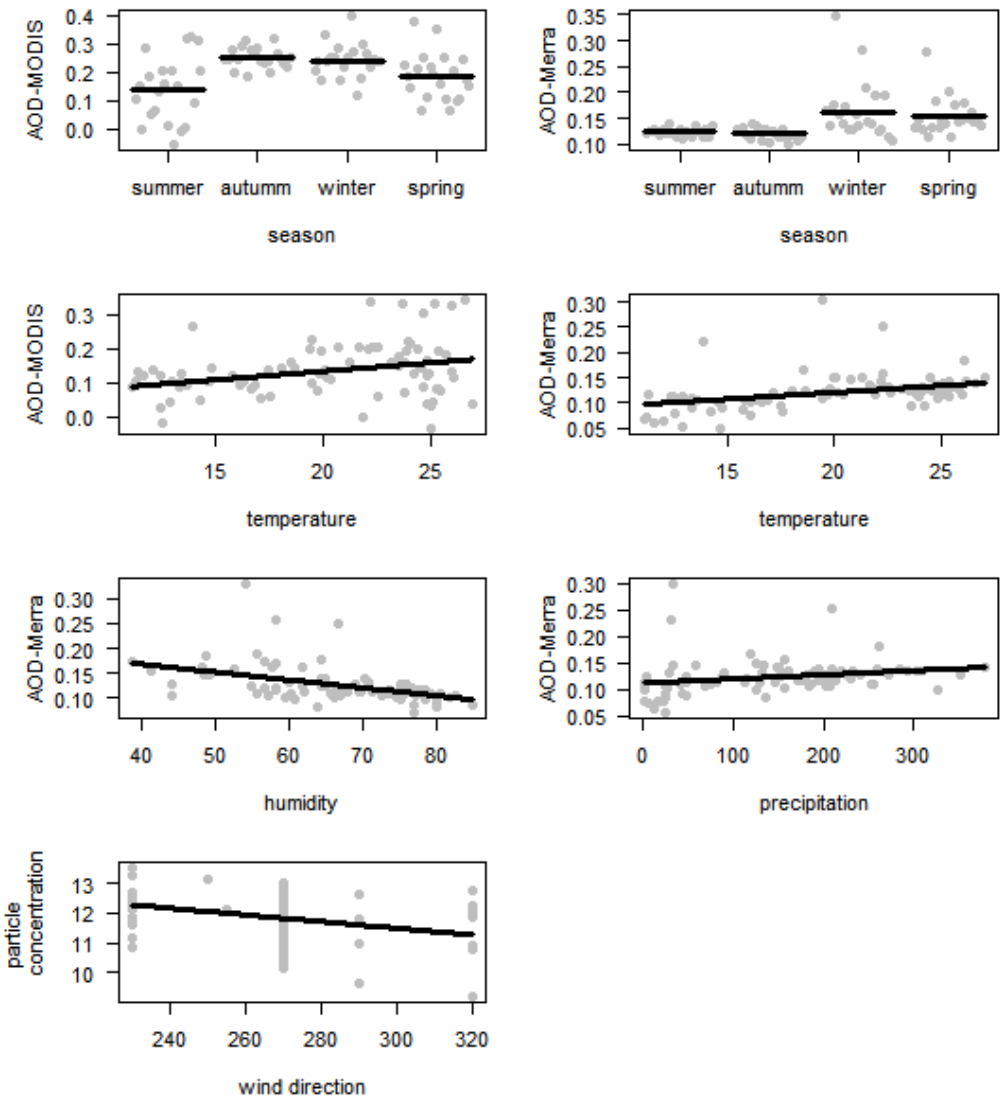

Figure 6. Direct influence of climatic variables and seasonality on the particle concentration, AOD550(MODIS), and AOD-Merra2 in Tucumán city, Argentina. Wind direction is shown in circular degrees. The observed points (partial residuals) are shown in grey. The fitted line corresponds to the prediction from the selected GLS models and indicates partial regressions (the slopes indicate direct relationships and depict the magnitude of change controlling for other variables in the model).

Table 1. Summary of selected models of generalized-least-squares on particle concentration (A), AOD_{550}(MODIS) (B), and AOD_{550}(MERRA-2) (C) in San Miguel de Tucumán city. Each model reflects the best representation of the influence of local climatic factors on the particle concentration and AOD considering the autoregressive structure. See Methods for details. Significant explanatory variables are depicted in bold.

A. Particle concentration †

Parameter	Estimate	SE	*T*	*p*
Intercept	17.1044	3.275	5.223	<0.0001
Autumn	−0.0531	0.432	−0.123	0.9025
Winter	0.4600	0.567	−0.811	0.4198
Spring	0.4311	0.338	1.274	0.2066
Temperature	0.0023	0.042	0.545	0.5871
Humidity	0.0057	0.024	0.231	0.8176
Wind direction	**−0.0112**	**0.005**	**−2.216**	**0.0297**
Wind velocity	−0.2405	0.144	−1.665	0.1000
Precipitation	−0.0031	0.002	−1.464	0.1473

† Model: *log(particle concentration) ~ f(season, temperature, humidity, wind direction, wind velocity, precipitation)*
Correlation Structure: AR(1), $\varphi_1 \sim 0$, where AR(1) indicates an autorregresive process of order 1; and φ_1 is the corresponding parameter**.**

B. AOD_{550} (MODIS) ††

Parameter	Estimate	SE	*T*	*p*
Intercept	0.1124	0.253	0.444	0.6586
Autumn	**0.1124**	**0.036**	**3.165**	**0.0022**
Winter	**0.0980**	**0.043**	**2.283**	**0.0252**
Spring	0.0469	0.037	1.285	0.2026
Temperature	**0.0050**	**0.002**	**2.086**	**0.0404**
Humidity	−0.0008	0.002	−0.378	0.7063
Wind direction	−0.0006	0.0004	−1.662	0.1006
Wind velocity	0.0124	0.012	1.080	0.2837
Precipitation	0.00002	0.0002	0.123	0.9026

†† Model: *log(AOD_{550}) ~ f(season, temperature, humidity, wind direction, wind velocity, precipitation)*
Correlation Structure: ARMA(1,0), φ_1 = 0.204, where ARMA(1,0) indicates an autorregresive process of order AR(1), and φ_1 is the corresponding parameter.

Continued on next page

C. AOD_{550}(MERRA-2) ††

Parameter	Estimate	SE	*T*	*p*
Intercept	0.2222	0.0665	3.342	0.0013
Autumn	−0.0033	0.0067	−0.490	0.6254
Winter	**0.0396**	**0.0164**	**2.423**	**0.0178**
Spring	**0.0295**	**0.0103**	**2.873**	**0.0053**
Temperature	**0.0027**	**0.0007**	**3.750**	**0.0003**
Humidity	**-0.0016**	**0.0005**	**−3.090**	**0.0028**
Wind direction	−0.0002	0.0001	−1.906	0.0605
Wind velocity	−0.0007	0.0020	−0.326	0.7452
Precipitation	**0.00008**	**0.00003**	**2.475**	**0.0156**

†† Model: *log(*AOD_{550}(MERRA-2)*) ~ f(season, temperature, humidity, wind direction, wind velocity, precipitation)*
Correlation Structure: ARMA(1,0), φ_1 = 0.127, where ARMA(1,0) indicates an autorregresive process of order AR(1), and φ_1 is the corresponding parameter.

When the type of the aerosol was considered, we detected that the variation in sulfates was significantly affected by temperature (estimate = 0.0014, SE = 0.0003, T = 4.251, p = 0.0001), humidity (estimate = 0.0006, SE = 0.0002, T = 3.198, p = 0.0020), precipitation (estimate = 0.00004, SE = 0.00002, T = 2.070, p = 0.0419) and wind direction (estimate = −0.0001, SE = 0.00004, T = −2.550, p = 0.0128). In the case of sea salt, their variation was explained by seasonal autumn effects (estimate = −0.0027, SE = 0.0007, T = −3.873, p = 0.0002), and humidity effects (estimate = 0.0001, SE = 0.00004, T = 2.177, p = 0.0326). The variation in organic carbon was significantly affected by seasonal effects in winter (estimate = 0.0348, SE = 0.0124, T = 2.805, p = 0.0064) and spring (estimate = 0.0267, SE = 0.0087, T = 3.066, p = 0.0030). Also, the variation in organic carbon was affected by temperature (estimate = 0.0012, SE = 0.0003, T = 3.854, p = 0.0002), humidity (estimate = −0.0015, SE = 0.0003, T = −5.236, p < 0.0001), precipitation (estimate = 0.00003, SE = 0.00002, T = 2.148, p = 0.0349), and wind velocity (estimate = −0.0025, SE = 0.0011, T = −2.179, p = 0.0325). The variation in black carbon was also explained by seasonal effects in winter (estimate = 0.0081, SE = 0.0026, T = 3.087, p = 0.0028) and spring (estimate = 0.0052, SE = 0.0017, T = 3.139, p = 0.0024), and by humidity effects (estimate = −0.0003, SE = 0.0001, T = −6.048, p < 0.0001). Finally, the variation in dust was affected by humidity (estimate = −0.0002, SE = 0.0001, T = −2.039, p = 0.0450). In summary, sulfates and sea salt were affected in a different way compared with carbon and dust. These different ways involve a notable seasonal effect, revealed also by the previous analyses, and the prevalent effects of climatic factors.

The fitting of GAM models revealed that AOD_{550}(MODIS) marginally affected the variation in particle concentration in a nonlinear way described by the s(MODIS, 1.87) residual function in Figure 7, where MODIS stands for AOD_{550}(MODIS) and 1.87 corresponds to the degrees of freedom (F_1 = 4.097, p = 0.0514). Concerning the slope of the AOD_{550}(MODIS), for values lower than 0.1 the relationship between this value and the particle concentration was negative and with high variability, while at values of AOD_{550}(MODIS) higher than 0.3, this relationship was positive and with minor variability. In the case of AOD_{550}(MERRA-2) series, non-linear effects on particle concentration were not significant (F_1 = 1.684, p = 0.1984). This result, together with the results from GLS models, support that AOD_{550}(MODIS) influences particle concentration variation by means of nonlinear dynamics driven by seasonality.

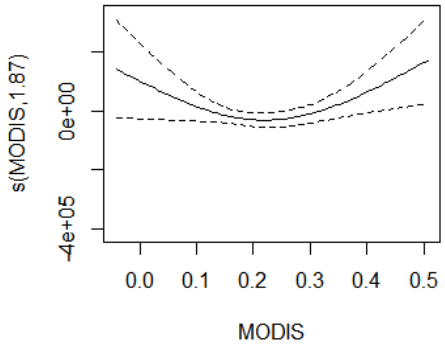

Figure 7. Estimated regression line with standard errors (broken lines) for the generalized additive mixed model for the influence of AOD550(MODIS) on particle concentration. The fitted line corresponds to partial regression (values on the vertical axis are residuals). Note the nonlinear effects of AOD550(MODIS) on particle concentration regardless of other factors (temperature, humidity, wind direction, wind velocity and precipitation).

5. Discussion and conclusions

This is the first study on the dynamics of atmospheric aerosols carried out for San Miguel de Tucumán city (Argentina Northwest) and its surrounding region, during a period of seven years. The results reveal that the aerosols, mainly dominated by small particles ($\leq$2.5 μm^2), depend mainly on climatic variables and human activities, which jointly contribute to the occurrence of a seasonal pattern in aerosol behavior in the place. In addition, the mean particle concentration shows a positive trend in the studied period. The space-time distribution of aerosols on a monthly basis at the regional scale depicts a sustained seasonal pattern of aerosol particles. A similar seasonal behavior is also observed for the particle concentration measured in-situ at the Tucumán city site. The seasonal effect is especially important for spring time, where anthropogenic aerosols related to the sugar cane activity increase. The importance of burning biomass in the atmospheric aerosol charge during sugar cane harvest is also evidenced by the large increase in Organic and Black Carbon during late winter and spring.

Given the environmental relevance of the atmospheric aerosols and their effect on human health, the significant trend in particle concentration deserves attention in terms of air monitoring and particle analysis. These near surface aerosols in San Miguel de Tucumán city are linked with the dry season (winter-spring), which is also the period when increased manufacturing activity takes place in Tucumán Province [22]. On the other hand, the lowest aerosol levels occur at the end of summer and beginnings of autumn, when sulfates are the dominant component of AOD. At the end of winter, the practice of sugarcane and citrus plants debris burning is very usual [23,62] and contributes to the load of solid particles to the atmosphere, among which organic carbon and carbon black particles predominate. Previous studies in this region [22] showed that the Aerosol Index (IA) increases strongly in the dry period and the aerosol particles deposited on plants leaves affect photosynthesis, with a negative impact of between 15% and 44%, depending on the considered species.

Large variations in the mean monthly particle concentration, as well as the occurrence of peak values, may be associated with sporadic dry and warm regional winds, locally called *zonda* or *argentinean* wind, that drag many atmospheric particles to the Tucumán region [26]. This premise is also supported by the fact that winds from west direction are more variable. Consequently, wind

direction and speed influence particle concentration at the local scale, while the AOD series was significantly affected by seasonality, and temperature. Since Tucumán city is placed in a valley (mean altitude of 450 m a.s.l and in the vicinity of a high slope West mountain of 625 m/km) the distribution, accumulation and deposition of solid particles is indirectly influenced by topography, which determines the speed and direction of winds and temperature. Future studies will focus on the aerosol characterization to evaluate whether there are new sources of aerosols in the region in addition to those reported in the mentioned bibliography and the MERRA-2 model. Altogether, our study remarks the importance of considering monitoring schemes at the local level in correspondence with remote sensing data, in order to obtain a deeper understanding of the atmospheric aerosols space-time dynamics. Also, the determinant climatic and anthropogenic factors on aerosol concentration and their environmental consequences should be a central focus of research in order to improve health policies [10,63,64]. A more detailed analysis on wind and space-time variation of aerosol dynamics of higher order over the region will be the focus of future research, in order to better understand the dynamics of aerosols in this region and the potential predictive value of satellite data.

The importance of the results presented in this work and the future research is in consonance with the 2016 World Health Organization Report [64] which emphasizes that: *air pollution—both ambient (outdoor) and household (indoor)—is the biggest environmental risk to health, carrying responsibility for about one in every nine deaths annually. Ambient (outdoor) air pollution alone kills around 3 million people each year, mainly from non-communicable diseases. Only one person in ten lives in a city that complies with the WHO Air quality guidelines. Air pollution continues to rise at an alarming rate and affects economies and people's quality of life; it is a public health emergency.* Since San Miguel de Tucumán and nearby cities do not have an official air pollution measurement system that can detect significant contamination episodes, the present (ground and satellite) results done for particulate matter (one of the main components of air pollution) will be provided to the cities and province authorities, in order that they can take appropriate protection measures for their human populations.

Acknowledgements

This work was performed within the CONICET PIP 0405 project. Data were obtained from samples from the air monitoring carried out by the Laboratorio de Palinología of the Fundación Miguel Lillo, led by Dr. María Elena García. Also, the authors acknowledge Gustavo Gudiño, Hebe Carreras and Beatriz Toselli for suggested comments and reference data. Analyses and visualizations of remote sensing data used in this work were produced with the Giovanni online data system, developed and maintained by the NASA GES DISC.

Conflicts of interest

The authors declare no conflicts of interest.

References

1. Davies SJ, Unam L (1999) Smoke-haze from the 1997 Indonesian forest fires: effects on pollution levels, local climate, atmospheric CO2 concentrations, and tree photosynthesis. *Forest Ecol Manag* 124: 137–144.

2. Rai PK, Panda LLS (2014) Leaf dust deposition and its impact on biochemical aspect of some roadside plants of Aizawl, Mizoram, North East India. *Int Res J Environ Sci* 3: 14–19.
3. Pope CA III, Burnett RT, Michael D, et al. (2002) Lung cancer, cardiopulmonary mortality, and long-term exposure to fine particulate air pollution. *J Amer Med Assoc* 287: 1132–1141.
4. Shah ASV, Lee KK, McAllister DA, et al. (2015) Short term exposure to air pollution and stroke: systematic review and meta-analysis. *BMJ* 350: h1295.
5. Sun X, Luo X, Zhao C, et al. (2015) The association between fine particulate matter exposure during pregnancy and preterm birth: a meta-analysis. *BMC Pregnancy Childbirth* 15: 300.
6. Ye X, She B, Benya S (2018) Exploring Regionalization in the Network Urban Space. *J Geovisual Spatial Analysis* 2: 4.
7. Atkinson RW, Mills IC, Walton HA, et al. (2015) Fine particle components and health—a systematic review and meta-analysis of epidemiological time series studies of daily mortality and hospital admissions. *J Expo Sci Env Epid* 25: 208–214.
8. Csavina J, Field J, Félix O, et al. (2014) Effect of wind speed and relative humidity on atmospheric dust concentrations in semi-arid climates. *Sci Total Environ* 487: 82–90.
9. Grobéty B, Gieré R, Dieze V, et al. (2010) Airborne particles in the urban environment. *Elements* 6: 229–234.
10. Kumar P, Hopke PK, Raja S, et al. (2012) Characterization and heterogeneity of coarse particles across an urban area. *Atmos Environ* 46: 449–459.
11. Achad M, López ML, Ceppi S, et al. (2014) Assessment of fine and sub-micrometer aerosols at an urban environment of Argentina. *Atmos Environ* 92: 522–532.
12. Arkouli M, Ulke AG, Endlicher W, et al. (2010) Distribution and temporal behavior of particulate matter over the urban area of Buenos Aires. *Atmos Pollut Res* 1: 1–8.
13. Escribano J, Gallardo L, Rondanelli R, et al. (2014) Satellite retrievals of aerosol optical depth over a subtropical urban area: the role of stratification and surface reflectance. *Aerosol Air Qual Res* 14: 596–607.
14. Garcia-Chevesich PA, Alvarado S, Neary DG, et al. (2014) Respiratory disease and particulate air pollution in Santiago Chile: Contribution of erosion particles from fine sediments. *Environ Pollut* 187: 202–205.
15. Ipiña A, Salum GM, Crino E, et al. (2012) Satellite and ground detection of very dense smoke clouds produced on the islands of the Paraná river delta that affected a large region in Central Argentina. *Adv Space Res* 49: 966–977.
16. Piacentini RD, García B, Micheletti MI, et al. (2016) Selection of astrophysical/astronomical/solar sites at the Argentina East Andes range taking into account atmospheric components. *Adv Space Res* 57: 2559–2574.
17. Micheletti MI, Louedec K, Freire M, et al. (2017) Aerosol concentration measurements and correlations with particle trajectories at the Pierre Auger Observatory. *Eur Phys J Plus* 132: 245.
18. Strawbridge KB, Snyder BJ (2004) Planetary boundary layer height determination during Pacific 2001 using the advantage of a scanning lidar instrument. *Atmos Environ* 38: 5861–5871.
19. Zhang Q, Quan J, Tie X, et al. (2011) Impact aerosol particles on cloud formation: Aircraft measurements in Beijing China. *Atmos Environ* 45: 665–672.
20. Finlayson-Pitts BJ, Pitts Jr JN, *Chemistry of the upper and lower atmosphere: theory, experiments, and applications*. Elsevier, 1999.

21. Zhang Q, Ma X, Tie X, et al. (2009) Vertical distributions of aerosols under different weather conditions: Analysis of in-situ aircraft measurements in Beijing, China. *Atmos Environ* 43: 5526–5535.
22. González JA, Prado FE, Piacentini RD (2014) Atmospheric dust accumulation on native and non-native species: Effects on gas exchange parameters. *J Environ Qual* 43: 801–808.
23. Benedetti PE (2014) Seguimiento de fuegos en Tucumán. Informe Nº 1. Instituto Nacional de Tecnología Agropecuaria, Centro Regional Tucumán—Santiago del Estero, Estación Experimental Agropecuaria Famaillá, Tucumán, Argentina. Available from: http://inta.gob.ar/documentos/seguimiento-de-fuegos-en-tucuman [In Spanish].
24. Sayago J, Collantes M, Toledo M (1998) Geomorfología, In: Gianfrancisco J. et al., editors, *Geología del Tucumán*. Publicación Especial Colegio de Graduados en Ciencias Geológicas de Tucumán: 241–258.
25. Sesma P, Guido E, Puchulu M (1998) Clima de la provincia de Tucumán. In: J. Gianfrancisco et al., editors, *Geología del Tucumán*. Publicación Especial Colegio de Graduados en Ciencias Geológicas de Tucumán, 41–46.
26. Minetti JL (2005) Climatología de los vientos, In: Minetti, J.L. editor, *El clima del noroeste argentino*. Laboratorio Climatológico Sudamericano. Fundación Carl C. zon Caldenius, Tucumán, Argentina, 117–127.
27. Hirst J (1952) An automatic volumetric spore trap. *Ann Appl Biol* 39: 257–265.
28. Aira MJ, Jato V, Iglesias I (2005) *Calidad del aire. Polen y esporas en la Comunidad Gallega*. España: Eds. Xunta de Galicia, Consellería de Medio Ambiente.
29. Rasband W (1997) *ImageJ*. National Institutes of Health, USA. Available from: http://rsb.info.nih.gov/ij/.
30. Shumway RH, Stoffer DS (1982) An approach to time series smoothing and forecasting using the EM algorithm. *J Time Ser Anal* 3: 253–264.
31. Ordano M, Engelhard I, Rempoulakis P, et al. (2015) Olive fruit fly (*Bactrocera oleae*) population dynamics in the Eastern Mediterranean: influence of exogenous uncertainty on a monophagous frugivorous insect. *PloS one* 10: e0127798.
32. Remer LA, Kaufman YJ, Tanré D, et al. (2005) The MODIS Aerosol algorithm, products, and validation. *J Atmos Sci* 62: 947–973.
33. GMAO—Global Modeling and Assimilation Office (2015) MERRA-2 tavgM_2d_aer_Nx: 2d, Monthly mean, Time-averaged, Single-Level, Assimilation, Aerosol Diagnostics V5.12.4, Greenbelt, MD, USA, Goddard Earth Sciences Data and Information Services Center (GES DISC).
34. Theil H (1950) A rank-invariant method of linear and polynomial regression analysis. *Nederlandse Akademie Wetenchappen Series A* 53: 386–392.
35. Sen PK (1968) Estimates of the regression coefficient based on Kendall's tau. *J Am Stat Assoc* 63: 1379–1389.
36. Box GEP, Jenkins GM, Reinsel GC (2008) *Time series analysis: forecasting and control*. Fourth edition, Hoboken, NJ: John Wiley & Sons, Inc.
37. Pinheiro JC, Bates DM (2000) *Mixed-effects models in S and S-PLUS*. New York: Springer-Verlag, Inc.
38. Venables WN, Ripley BD (2002) *Modern applied statistics with S*. New York: Springer.

39. Zuur AF, Ieno EN, Walker NJ, et al. (2009) *Mixed effects models and extensions in ecology with R*. New York: Springer Science+Business Media, LLC.
40. Gałecki AT, Burzykowski T (2013) *Linear mixed-effects models using R. A step-by-step approach*. New York: Springer Science & Business Media.
41. Fox J, Weisberg S (2011) *An R companion to applied regression*. Second edition, Thousand Oaks: Sage.
42. Hastie TJ, Tibshirani RJ (1990) *Generalized additive models*. Boca Raton, FL: Chapman & Hall/CRC.
43. R Development Core Team (2017) R: A Language and Environment for Statistical Computing. R Foundation for Statistical Computing, Vienna, Austria. Available from: http://www.R-project.org/
44. Agostinelli C, Lund U, *R package 'circular': Circular Statistics* (version 0.4-7)[Computer software], (2013). Available from: https://r-forge.r-project.org/projects/circular/
45. Højsgaard S, Halekoh U, Robison-Cox J, et al. (2013) *doBy: doBy - Groupwise summary statistics, LSmeans, general linear contrasts, various utilities*. R package version 4.5–10. Available from: http://CRAN.R-project.org/package=doBy
46. Hyndman RJ, Khandakar Y, Automatic time series forecasting: the forecast package for R. Monash University, Department of Econometrics and Business Statistics, 2007.
47. Wickham H, ggplot2: elegant graphics for data analysis. Springer, 2016.
48. Sarkar D, Andrews F, *latticeExtra: Extra graphical utilities based on Lattice*. R package version 0.6-26, 2013. Available from: http://CRAN.R-project.org/package=latticeExtra
49. Wood SN (2004) Stable and efficient multiple smoothing parameter estimation for generalized additive models. *J Am Stat Assoc* 99: 673–686.
50. Pinheiro J, Bates D, DebRoy S, et al. (2015) *nlme: Linear and nonlinear mixed effects models*. R package version 3.1–122, Available from: http://CRAN.R-project.org/package=nlme.
51. Carslaw DC, Ropkins K (2012) openair—an R package for air quality data analysis. *Environ Modell Softw* 27: 52–61.
52. Breheny P, Burchett W (2015) *visreg: Visualization of regression models*. R package version 2.2-0. Available from: http://CRAN.R-project.org/package=visreg
53. Christopher SA, Wang M, Berendes TA, et al. (1998) The 1985 Biomass Burning Season in South America: Satellite Remote Sensing of Fires, Smoke, and Regional Radiative Energy Budgets. *J Appl Meteor* 37: 661–678.
54. Castro Videla F, Barnaba F, Angelini F, et al. (2013) The relative role of Amazonian and non-Amazonian fires in building up the aerosol optical depth in South America: A five year study (2005–2009). *Atmospheric Research* 122: 298–309.
55. Filonchyk M, Yan H, Yang S, et al. (2017) Detection of aerosol pollution sources during sandstorms in Northwestern China using remote sensed and model simulated data. *Adv Space Res*.
56. Filonchyk M, Yan H, Shareef TME, et al. (2018) Aerosol contamination survey during dust storm process in Northwestern China using ground, satellite observations and atmospheric modeling data. *Theor Appl Climatol*, 1–15.
57. Liu Y, Franklin M, Kahn R, et al. (2007) Using aerosol optical thickness to predict ground-level PM2.5 concentrations in the St. Louis area: A comparison between MISR and MODIS. *Remote Sens Environ* 107: 33–44.

58. Kahn RA, Gaitley BJ, Martonchik JV, et al. (2005) Multiangle Imaging Spectroradiometer (MISR) global aerosol optical depth validation based on 2 years of coincident Aerosol Robotic Network (AERONET) observations. *J Geophys Res* 110(D10).
59. Hu Z (2009) Spatial analysis of MODIS aerosol optical depth, PM 2.5, and chronic coronary heart disease. *Int J Health Geogr* 8: 27.
60. Li Y, Chen Q, Zhao H, et al. (2015) Variations in PM 10, PM 2.5 and PM 1.0 in an urban area of the Sichuan Basin and their relation to meteorological factors. *Atmosphere* 6: 150–163.
61. van Donkelaar A, Martin RV, Park RJ. (2006) Estimating ground-level PM2.5 using aerosol optical depth determined from satellite remote sensing. *J Geophys Res Atmos* 111(D21).
62. Tonatto MJ, Fernández de Ullivarri J, Alonso JM, et al. (2008) Sugarcane burning teledetection through MODIS system in Tucumán (Argentina). *Revista Industrial y Agrícola de Tucumán* 85: 31–35.
63. Carreras HA, Wannaz ED, Pignata ML (2009) Assessment of human health risk related to metals by the use of biomonitors in the province of Córdoba, Argentina. *Environ Pollut* 157: 117–122
64. García ME (2010) Aeropalinología de la ciudad de Yerba Buena, provincia de Tucumán (Argentina). *Acta Botánica Malacitana* 35: 115–131.
65. WHO (World Health Organization), Ambient air pollution: A global assessment of exposure and burden of disease. Published by WHO Document Production Services, Geneva, Switzerland. 2016. Available from: http://apps.who.int/iris/bitstream/10665/250141/1/9789241511353-eng.pdf.

AIMS Press